

# Earth matter effect on GeV neutrino propagation

Yaithd Daniel Olivas Arcos, Sarira Sahu

*Instituto de Ciencias Nucleares, Universidad Nacional Autónoma de México,  
Circuito Exterior, C.U., A. Postal 70-543, 04510 Mexico DF, Mexico*

We have studied the Earth matter effect on the oscillation of upward going GeV neutrinos by taking into account the three active neutrino flavors. For neutrino energy in the range 3 to 12 GeV we observed three distinct resonant peaks for the oscillation process  $\nu_e \leftrightarrow \nu_{\mu,\tau}$  in three *distinct* densities. For the calculation of observed flux of these GeV neutrinos, we considered two different flux ratio at the source, the standard scenario with flux ratio 1 : 2 : 0 and the muon damped scenario 0 : 1 : 0. It is observed that while the standard scenario gives the observed flux ratio 1 : 1 : 1, the muon damped scenario has a different ratio. The PINGU will be able to shed more light on the nature of the resonance in these GeV neutrinos.

## INTRODUCTION

During the last couple of decades, a significant amount of information about the neutrino properties have been obtained by many experiments[1–5] and now neutrino physics has entered an era of precision measurement and deeper understanding of the oscillation phenomena. The recent observation of TeV-PeV neutrino events by IceCube in South Pole for the first time shows the cosmological origin of these high energy neutrinos[6, 7], although the sources and the production mechanism are still unknown. The DeepCore subarray[8] of the IceCube has the energy threshold of about 10 GeV which can study low energy neutrino physics. Also below 100 GeV the DeepCore increases the effective area of IceCube by more than an order of magnitude. So the DeepCore subarray has opened a new window on GeV neutrino oscillation physics, mostly the atmospheric neutrino oscillation. The next generation upgrade to IceCube is the Precision IceCube Next Generation Upgrade (PINGU) [9]. This will deploy an additional 20 strings within the DeepCore to lower the sensitivity from  $\mathcal{O}(10)$  GeV to  $\mathcal{O}(1)$  GeV. The goal of PINGU is to perform precise measurements of atmospheric neutrino oscillations down to a few GeV and to determine the neutrino mass hierarchy.

The matter effect on the neutrino oscillations is being studied in different context[10–15]. The neutrino properties get modified due to the medium effect. Even a massless neutrino acquires an effective mass and an effective potential in the matter. When the neutrinos from the interior of the sun propagate out, they can undergo resonant conversion from one flavor to another due to the medium effect which is well known as the Mikheyev-Smirnov-Wolfenstein (MSW) effect[16, 17]. Similarly, the neutrino propagation in the supernova medium[18], in Gamma-Ray Burst (GRB) fireball[19, 20], in Choked GRBs[21, 22] and early universe hot plasma[23] can have many important implications in their respective physics. The neutrino propagation in the Earth has also been studied in various context and different approximation to the Earth density profile are considered [14, 15, 24]. For most of the realistic calculations, the Preliminary Ref-

erence Earth Model (PREM)[25] density profile is considered. In this case the density obtained is function of depth from the surface of the Earth and both longitudinal and latitudinal variations are ignored. Also the density profile of the Earth is symmetric on both sides of the centre of the Earth. All oscillation experiments of same baseline length will have the same matter effect.

Apart from the atmospheric neutrinos, there are other astrophysical objects which produce multi-GeV neutrinos, for example, GRBs[26, 27], and AGN[28]. So it is interesting to study the matter effect on the oscillation of these neutrinos when crossing the diameter of the Earth and modification in their flux ratios. We have shown that the Earth matter effect produces three resonances between 3 to 12 GeV neutrino energy. Due to the lower sensitivity of the PINGU, it will be able to probe these resonances.

Here we would like to consider the three flavor model to study the Earth matter effect on the upward going neutrinos and the possible modification of their flux ratio at the detector. The paper is organized as follows: In Sec. 2 we discuss about the formalism used to calculate the neutrino oscillation probability in the presence of matter background. The discussion about the realistic Earth density profile is done in Sec. 3. In Sec. 4 we elaborate about our results and a comprehensive discussion is given in Sec. 5.

## FORMALISM

The neutrino oscillation in vacuum and matter has been discussed extensively for solar, atmospheric, as well as accelerator and reactor experiments. Models of three active flavor neutrinos oscillation in constant matter density[29–31], linearly varying density and exponentially varying density have been studied[32, 33]. In Ref.[13] T. Ohlsson and H. Snellman have developed an analytic formalism for the oscillation of three flavor neutrinos in the matter background with varying density, where they use the plane wave approximation for the neutrinos (henceforth we refer to this as OS formalism).

Here the evolution operator and the transition probabilities are expressed as functions of the vacuum mass square differences, vacuum mixing angles and the matter density parameter. As application of the above formalism, the authors have studied the neutrino oscillations traversing the Earth and the Sun for constant, step-function and varying matter density profiles[14, 15]. To handle the varying density, the distance is divided into equidistance slices and in each slice the matter density is assumed to be constant. Recently this formalism is also used to study the multi-TeV neutrino propagation in the choked GRBs[22] and the calculation of the track to shower ratio of the multi-TeV neutrinos in IceCube[34]. In this sec-

tion we review the OS formalism for the calculation of neutrino oscillation probability.

In the context of three active neutrino flavors, a flavor neutrino state can be expressed as a linear superposition of mass eigenstates as

$$|\nu_\alpha\rangle = \sum_{i=1}^3 U_{\alpha i}^* |\nu_i\rangle, \quad (1)$$

where  $\alpha = e, \mu, \tau$  (flavor eigenstates) and  $i = 1, 2, 3$  (mass eigenstates). The  $U_{\alpha i}$  is the three by three neutrino mixing matrix given by,

$$U = \begin{pmatrix} U_{e1} & U_{e2} & U_{e3} \\ U_{\mu 1} & U_{\mu 2} & U_{\mu 3} \\ U_{\tau 1} & U_{\tau 2} & U_{\tau 3} \end{pmatrix} = \begin{pmatrix} c_{13}c_{12} & c_{13}s_{12} & s_{13}e^{-i\delta_{cp}} \\ -s_{12}c_{23} - c_{12}s_{23}s_{13}e^{i\delta_{cp}} & c_{12}c_{23} - s_{12}s_{23}s_{13}e^{i\delta_{cp}} & s_{23}c_{13} \\ s_{23}s_{12} - c_{23}s_{13}c_{12}e^{i\delta_{cp}} & -s_{23}c_{12} - s_{13}s_{12}c_{23}e^{i\delta_{cp}} & c_{23}c_{13} \end{pmatrix}, \quad (2)$$

where  $c_{ij} \equiv \cos\theta_{ij}$  and  $s_{ij} \equiv \sin\theta_{ij}$  for  $i, j = 1, 2, 3$ . With three neutrino flavors, there are three neutrino mixing angles  $\theta_{12}, \theta_{13}, \theta_{23}$  and CP violating phase  $\delta_{CP}$ . In the present analysis we take  $\delta_{CP} = 0$  since CP non conservation is negligible at the present level of accuracy hence the entries of the CKM matrix are real numbers.

Propagating neutrinos in a medium experience an effective potential due to the collision with the particles in the background matter. Depending on the neutrino flavor the interaction can be charged current (CC) or neutral current (NC) or both. The neutral current interaction is same for all the neutrinos which can be factored out as a global phase and only charged current term will contribute. This is attributed only to electron neutrino and its anti-neutrinos. The effective potential is expressed as

$$V_f = A \begin{pmatrix} 1 & 0 & 0 \\ 0 & 0 & 0 \\ 0 & 0 & 0 \end{pmatrix}, \quad (3)$$

where  $A = \pm\sqrt{2}G_F N_e$ ,  $G_F$  is the Fermi coupling constant and  $N_e$  represents the electron number density in the background medium and signs  $\pm$  correspond to  $\nu_e$  and  $\bar{\nu}_e$  respectively.

In vacuum, the Hamiltonian that described the propagation of the neutrinos in the mass eigenstate basis is described by

$$H_m = \begin{pmatrix} E_1 & 0 & 0 \\ 0 & E_2 & 0 \\ 0 & 0 & E_3 \end{pmatrix}, \quad (4)$$

where  $E_i$ , for  $i = 1, 2, 3$  refer to the energy of each neutrino mass eigenstate with

$$E_i = \sqrt{\mathbf{p}^2 + m_i^2}. \quad (5)$$

Here we assume that neutrinos with different masses have the same momentum. This Hamiltonian can be written in the flavor basis through the unitary transformation described by the matrix  $U$  from equation (2), as

$$H_f = U H_m U^{-1}. \quad (6)$$

In the mass basis, the total Hamiltonian is given by

$$\begin{aligned} \mathcal{H}_m &= H_m + U^{-1} V_f U \\ &= H_m + V_m. \end{aligned} \quad (7)$$

The total Hamiltonian in the flavor basis is written as

$$\mathcal{H}_f = H_f + V_f. \quad (8)$$

For neutrino propagation in a medium, the Hamiltonian is not diagonal, neither in the mass basis nor in the flavor basis, so one has to calculate the evolution operator in any of these basis. In the mass basis, the evolution of the state at a later time  $t$  will be obtained by solving the Schrödinger equation

$$i \frac{d|\nu_i(t)\rangle}{dt} = \mathcal{H}_m |\nu_i(t)\rangle, \quad (9)$$

and the solution to this equation can be expressed in terms of the evolution operator as

$$\begin{aligned} |\nu_i(t)\rangle &= e^{-i\mathcal{H}_m t} |\nu_i(0)\rangle \\ &= U_m(t) |\nu_i(0)\rangle, \end{aligned} \quad (10)$$

where  $U_m(t) = e^{-i\mathcal{H}_m t}$  is the evolution operator in the mass basis and in the flavor basis this can be written as

$$U_f(t) = U U_m(t) U^{-1}. \quad (11)$$

Neutrinos being relativistic, we can replace  $t$  by the path length  $L$ , where we use the natural units  $c = 1$  and  $\hbar = 1$ .

The evolution operator of Eq.(11) can be computed using the definition of the exponential of a matrix but it is not a straightforward task since the definition implies an infinite sum. The Cayley-Hamilton theorem provides a powerful tool to reduce this infinite sum to a finite sum and is given by

$$\begin{aligned} e^{-i\mathcal{H}_m t} &= e^{-iTt - \frac{i}{3}(Tr\mathcal{H}_m)It} \\ &= \phi e^{-iTt} \\ &= \phi [a_0 I + a_1(-iTt) + a_2(-iTt)^2] \\ &= \phi (a_0 I - ia_1 t T - a_2 t^2 T^2), \end{aligned} \quad (12)$$

where we define the traceless matrix  $T = \mathcal{H}_m - \frac{1}{3}Tr(\mathcal{H}_m)I$  and  $I$  is the identity matrix. The final expression for the evolution operator is given by (by replacing  $t$  to  $L$ )

$$e^{-i\mathcal{H}_m L} = \phi (a_0 I - ia_1 L T - a_2 L^2 T^2). \quad (13)$$

In order to determine the evolution operator it is necessary to know the coefficients  $a_i$  in Eq.(13). The  $T$  matrix has three eigenvalues  $\lambda_i$  with  $i = 1, 2, 3$  and the characteristic equation is

$$\lambda^3 + c_2 \lambda^2 + c_1 \lambda + c_0 = 0. \quad (14)$$

The coefficients of  $\lambda$  are given as

$$c_0 = -\det(T), \quad c_2 = -tr(T) = 0, \quad (15)$$

and

$$c_1 = T_{11}T_{22} - T_{12}^2 + T_{11}T_{33} - T_{13}^2 + T_{22}T_{33} - T_{23}^2. \quad (16)$$

This reduces the Eq.(17) to

$$\lambda^3 + c_1 \lambda + c_0 = 0, \quad (17)$$

and the eigenvalues are given as

$$\begin{aligned} \lambda_1 &= \frac{X}{2^{1/3}3^{2/3}} - \frac{(\frac{2}{3})^{1/3}c_1}{X}, \\ \lambda_{2,3} &= \frac{(1 \pm i\sqrt{3})c_1}{2^{2/3}3^{1/3}X} - \frac{(1 \mp i\sqrt{3})X}{2 \times 2^{1/3}3^{2/3}}, \end{aligned} \quad (18)$$

with

$$X = \left( \sqrt{3} \sqrt{4c_1^3 + 27c_0^2} - 9c_0 \right)^{1/3}. \quad (19)$$

With the use of the above equations, the evolution operator in the mass basis can be written as

$$\begin{aligned} U_m(L) &= e^{-i\mathcal{H}_m L} \\ &= \phi \sum_{a=1}^3 e^{-iL\lambda_a} \frac{[(\lambda_a^2 + c_1)I + \lambda_a T + T^2]}{3\lambda_a^2 + c_1}, \end{aligned} \quad (20)$$

The evolution operator in the flavor basis is given by

$$\begin{aligned} U_f(L) &= e^{-i\mathcal{H}_f L} \\ &= U e^{-i\mathcal{H}_m L} U^{-1} \\ &= \phi \sum_{a=1}^3 e^{-iL\lambda_a} \frac{[(\lambda_a^2 + c_1)I + \lambda_a \tilde{T} + \tilde{T}^2]}{3\lambda_a^2 + c_1}, \end{aligned} \quad (21)$$

where  $\tilde{T}$  is in the flavor basis.

The probability of flavor change from a flavor  $\alpha$  to another flavor  $\beta$  due to neutrino oscillation through a distance  $L$  can be given by

$$\begin{aligned} P_{\nu_\alpha \rightarrow \nu_\beta}(L) &\equiv P_{\alpha\beta}(L) = |\langle \nu_\beta | U_f(L) | \nu_\alpha \rangle|^2 \\ &= \delta_{\alpha\beta} - 4 \sum_{a=1}^3 \sum_{b=1}^3 P_a(L)_{\beta\alpha} P_b(L)_{\beta\alpha} \sin^2 x_{ab}, \end{aligned} \quad (22)$$

where we have defined

$$P_a(L)_{\beta\alpha} = \frac{(\lambda_a^2 + c_1)\delta_{\beta\alpha} + \lambda_a \tilde{T}_{\beta\alpha} + \tilde{T}_{\beta\alpha}^2}{3\lambda_a^2 + c_1}. \quad (23)$$

The matrices  $\tilde{T}_{\beta\alpha}$  and  $\tilde{T}_{\beta\alpha}^2$  are symmetric and defined as

$$\tilde{T}_{\alpha\beta} = \tilde{T}_{\beta\alpha} = \sum_{a=1}^3 \sum_{b=1}^3 U_{\alpha a} U_{\beta b} T_{ab}, \quad (24)$$

and

$$\tilde{T}_{\alpha\beta}^2 = \tilde{T}_{\beta\alpha}^2 = \sum_{a=1}^3 \sum_{b=1}^3 U_{\alpha a} U_{\beta b} T_{ab}^2. \quad (25)$$

Also we have defined the quantity

$$x_{ab} = \frac{(\lambda_a - \lambda_b)L}{2}. \quad (26)$$

The matrix  $T$  is written explicitly as

$$T_{ab} = \begin{pmatrix} T_{11} & AU_{e1}U_{e2} & AU_{e1}U_{e3} \\ AU_{e1}U_{e2} & T_{22} & AU_{e2}U_{e3} \\ AU_{e1}U_{e3} & AU_{e2}U_{e3} & T_{33} \end{pmatrix}, \quad (27)$$

where the diagonal elements of the above matrix are given by

$$T_{aa} = AU_{ea}^2 + \frac{1}{3} \left( \sum_{b \neq a=1}^3 E_{ab} - A \right). \quad (28)$$

Here  $E_{ab} = -E_{ba} = E_a - E_b$  and the energies satisfy the relation

$$E_{12} + E_{23} + E_{31} = 0. \quad (29)$$

The neutrino oscillation probabilities satisfy the condition

$$\sum_{\beta} P_{\alpha\beta} = 1, \text{ for } \alpha, \beta = e, \mu, \tau, \quad (30)$$

and a similar condition is satisfied for anti-neutrinos which we define as  $P_{\bar{\alpha}\bar{\beta}}$ .

Using the Eqs.(22) and (30) we can calculate the probability of transition from one flavor to another. For  $V_f = 0$ , we get the vacuum transition probability. For matter with varying density the distance  $L$  can be discretized into small intervals  $[L_i, L_{i+1}]$  in such a way that the density profile is almost constant in each segment and can be used this procedure repeatedly in each segment. By doing so we can study numerically the neutrino oscillation in any type of density profile. For neutrinos traversing a series of matter densities  $\rho_i$  for  $i = 1$  to  $n$ , with their corresponding thickness  $L_i$ , the total evolution operator is the ordered product and is given as

$$U_f(L) = \prod_i^n U_f(L_i), \quad (31)$$

---


$$\rho(x) = \begin{cases} 13.0885 - 8.8381x^2, & 0 \leq x \leq 0.191 \\ 12.5815 - 1.2638x - 3.6426x^2 - 5.5281x^3, & 0.191 < x \leq 0.546 \\ 7.9565 - 6.4761x + 5.5283x^2 - 3.0807x^3, & 0.546 < x \leq 0.895 \\ 5.3197 - 1.4836x, & 0.895 < x \leq 0.905 \\ 11.2494 - 8.0298x, & 0.905 < x \leq 0.937 \\ 7.1089 - 3.8045x, & 0.937 < x \leq 0.965 \\ 2.6910 + 0.6924x, & 0.965 < x \leq 0.996 \\ 2.900, & 0.996 < x \leq 0.997 \\ 2.600, & 0.997 < x \leq 0.999 \\ 1.020, & 0.999 < x \leq 1. \end{cases} \quad (32)$$


---

Here  $x = r/R_{\oplus}$ ,  $R_{\oplus} = 6367$  km is the radius of the Earth and the density  $\rho$  is in units of  $\text{g/cm}^3$  which is shown in Fig. 1 as a function of  $r$ . The density profile is symmetric around the centre of the Earth and independent of the longitudinal and latitudinal variations.

## RESULTS

In the standard picture of neutrino oscillations, the oscillation experiments with solar, atmospheric, reactor and accelerator neutrinos can be explained through the

where  $\sum_i^n L_i = L$ . In a series of papers by OS, this method has been applied for different density profiles of the Sun and the Earth, to study the MeV energy neutrino oscillation[13–15, 24].

## EARTH DENSITY PROFILE

High energy neutrinos reaching the detector like Ice-Cube from opposite side of the Earth can experience both oscillation and absorption due to CC and NC interactions. While the oscillation is important for low energy neutrinos  $E_{\nu} \leq 10$  TeV, for very high energy neutrinos the interaction cross sections are large so that the absorption effects become very important and have to be taken into account as the shadowing effect[34]. But here we are considering the multi-GeV neutrinos, so the absorption effect is very small and we don't take into account. Although, the density profile of the Earth is not known exactly, here we consider the the most realistic density profile PREM[25] which is given as

---

parameters[5, 35, 36]

$$\begin{aligned} \Delta m_{21}^2 &= 8.0 \times 10^{-5} \text{eV}^2, & \theta_{12} &= 33.8^\circ, & \theta_{23} &= 45^\circ \\ \Delta m_{31}^2 &= 3.2 \times 10^{-3} \text{eV}^2, & \theta_{13} &= 8.8^\circ & \text{and } \delta_{CP} &= (\text{83}) \end{aligned}$$

with  $\Delta m_{ij}^2 = m_i^2 - m_j^2$ . Throughout our analysis we will be using the above neutrino parameters. Here for our analysis we consider neutrinos in the energy range 1 – 100 GeV.

For  $\nu_e$  oscillating to  $\nu_{\mu}$  and  $\nu_{\tau}$  we can clearly see three distinct resonance peaks in three different neutrino energies  $E_{\nu}$  corresponding to three different densities  $\rho$  of the Earth. The oscillation probability  $P_{e\beta}$  is shown in

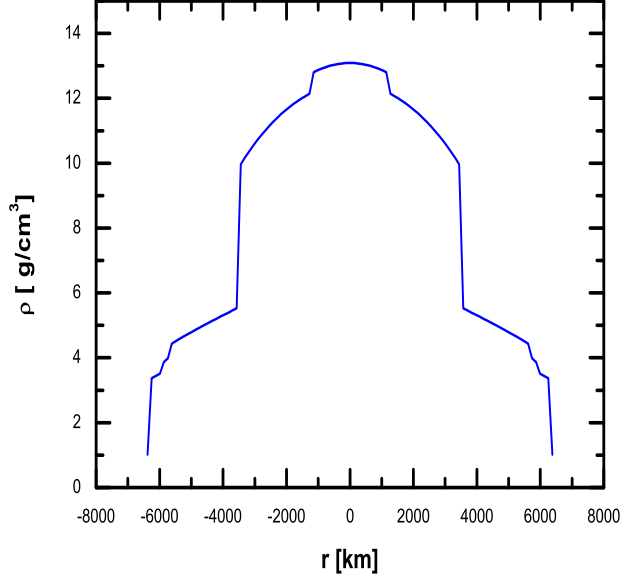


FIG. 1. The Earth density profile PREM is plotted as a function radius  $r$ .

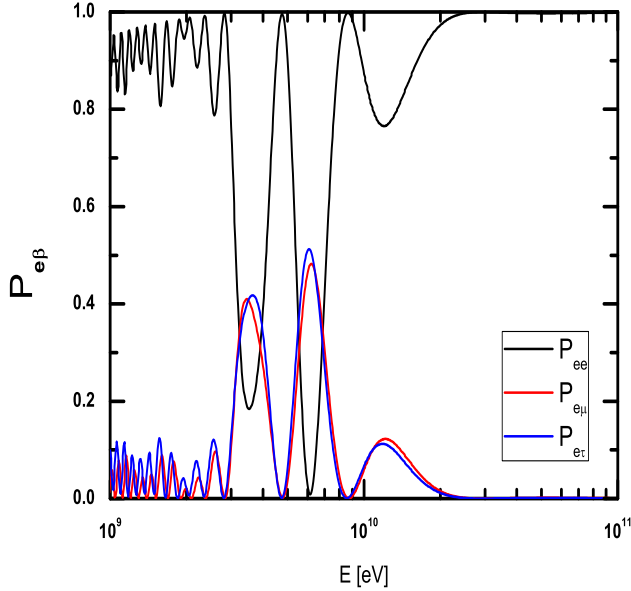


FIG. 2.  $P_{e\beta}$  as a function of neutrino energy  $E_\nu$ .

Fig. 2. For  $E_\nu = 3.45$  GeV, the resonance takes place deep in the core where  $\rho = 11.5 \text{ gm/cm}^3$  at a depth of  $\sim 2483$  km. The third peak is for  $E_\nu = 12.0$  GeV and the corresponding resonance density and the distance are respectively  $3.4 = \text{gm/cm}^3$  and  $6112$  km. These two peaks are clearly of MSW type because the resonance density

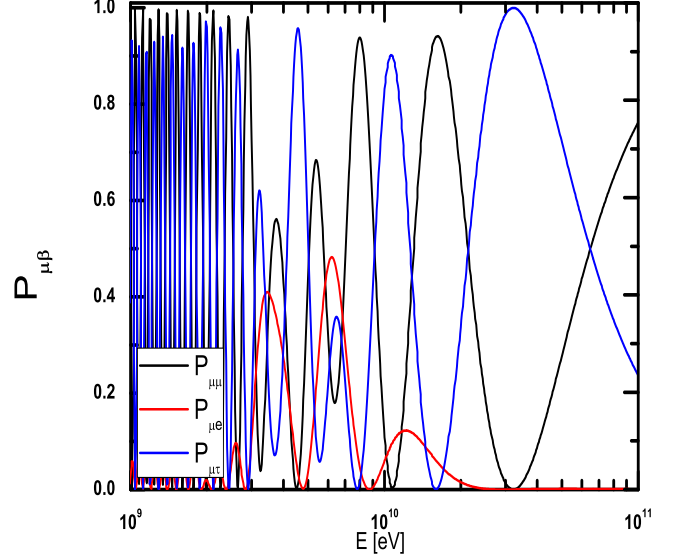


FIG. 3.  $P_{e\beta}$  as a function of neutrino energy  $E_\nu$ .

and the resonance length exist for these neutrinos. On the other hand, for the second peak with  $E_\nu = 6.18$  GeV, the resonance density  $\rho = 6.6 \text{ gm/cm}^3$  does not exist in the Earth's interior (Fig. 1). So this resonance can't be of MSW type. Below the first resonance peak ( $E_\nu < 3.45$  GeV) the probability is oscillatory in nature.

In Fig. 2 we have shown the  $P_{ee}$ ,  $P_{e\mu}$  and  $P_{e\tau}$  for  $1 \text{ GeV} \leq E_\nu \leq 100 \text{ GeV}$ . It shows that for both the oscillations  $\nu_e \leftrightarrow \nu_\mu$  and  $\nu_e \leftrightarrow \nu_\tau$ , the resonance peaks are at the same place for a given  $E_\nu$ . Beyond  $\sim 20$  GeV the transition probabilities are very small which implies that the Earth's matter does not play any significant role beyond this energy and the oscillation is purely due to the vacuum.

In Fig. 3 we have shown the  $P_{\mu\mu}$  and transition probabilities of muon neutrino to  $\nu_e$ ,  $P_{\mu e}$  and to  $\nu_\tau$ ,  $P_{\mu\tau}$ . The three resonance peaks in  $P_{\mu e}$  are clearly seen (red curve) but there is no resonant oscillation for  $\nu_\mu \leftrightarrow \nu_\tau$  (blue curve). Above about  $\sim 20$  GeV the  $P_{\mu e}$  goes to zero. The  $P_{\mu\mu}$  and  $P_{\mu\tau}$  are out of phase by  $180^\circ$ . We observed that for  $E_\nu > 100$  GeV the  $\nu_\mu$  does not oscillate to  $\nu_\tau$  any more. The oscillation process  $\nu_\tau \leftrightarrow \nu_e$  is same as  $\nu_e \leftrightarrow \nu_\mu$ , hence we do not discuss about it.

Due to the matter effect the energy eigenvalues of the neutrinos are given by  $\lambda_a$  and the energy difference is related to the effective mass square difference as

$$|\lambda_i - \lambda_j| = \frac{|\Delta \tilde{m}_{ij}^2|}{2E_\nu}. \quad (34)$$

In Fig. 4 we have plotted  $|\lambda_i - \lambda_j|$  as a function of Earth density  $\rho$  for resonance neutrino energy  $E_\nu = 3.45$  GeV.

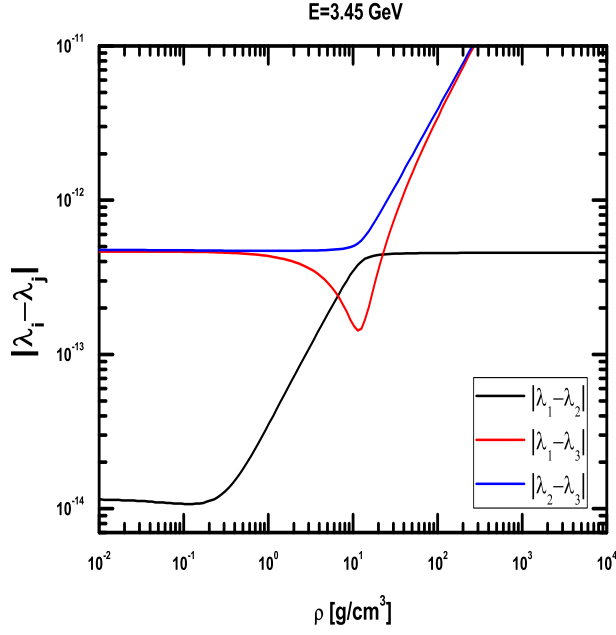


FIG. 4. Neutrino energy difference is plotted as a function of density

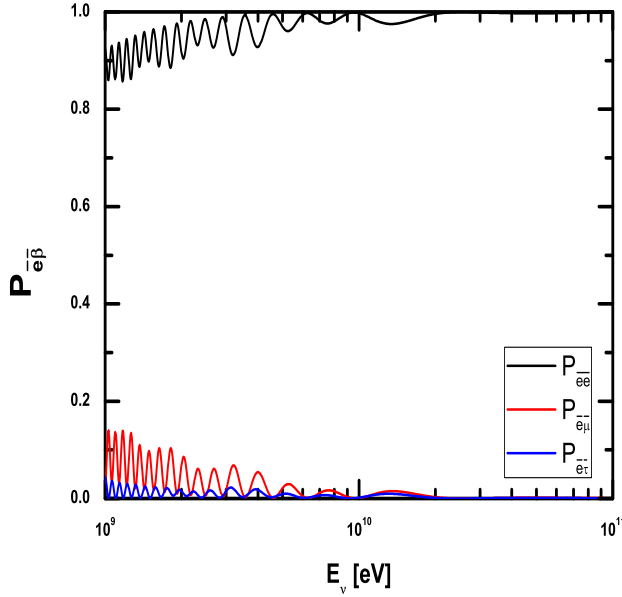


FIG. 5.  $P_{\bar{\mu}\beta}$  as a function of  $E_\nu$ .

It shows that, at the resonance density  $\rho_c$ , both  $|\lambda_1 - \lambda_2|$  and  $|\lambda_2 - \lambda_3|$  have the closest approach and at this point the neutrino mixing is maximal. Going from the resonance peak at 3.45 GeV to 12 GeV the resonance density decreases from  $11.5 \text{ g/cm}^3$  to  $3.4 \text{ g/cm}^3$ .

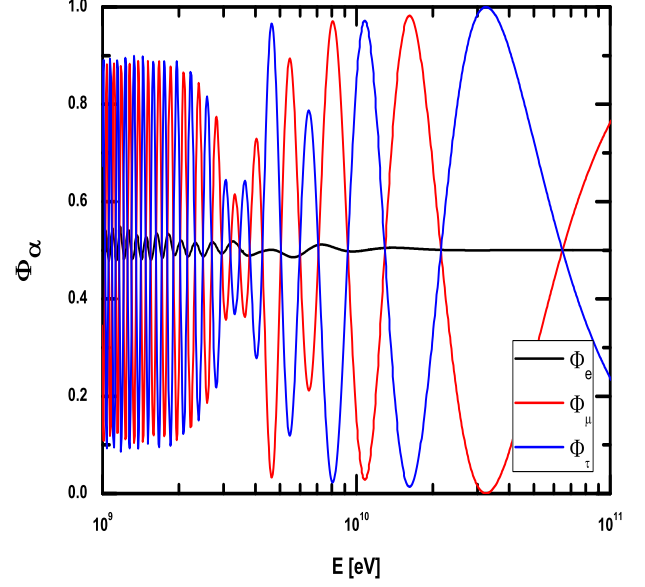


FIG. 6. Neutrino flux at the IceCube detector when  $\Phi_{\nu_e}^0 : \Phi_{\nu_\mu}^0 : \Phi_{\nu_\tau}^0 = 1 : 2 : 0$ .

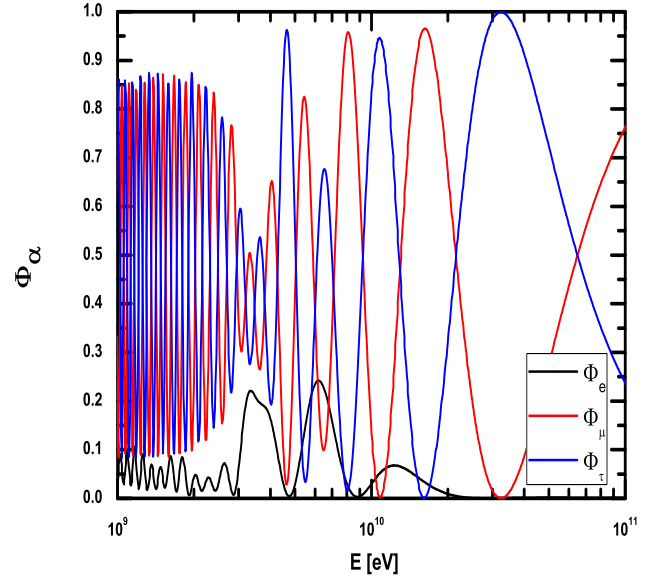


FIG. 7. Neutrino flux at the IceCube detector when  $\Phi_{\nu_e}^0 : \Phi_{\nu_\mu}^0 : \Phi_{\nu_\tau}^0 = 0 : 1 : 0$ .

We have also done the analysis for the oscillation of anti-neutrinos which are shown in Fig. 5. We observed that there is no resonant oscillation of the anti-neutrinos. In the low energy limit (between 1 to 10 GeV)

for  $\bar{\nu}_e \leftrightarrow \bar{\nu}_{\mu,\tau}$  oscillation, the oscillation of  $\bar{\nu}_e$  to  $\bar{\nu}_\mu$  is more preferable than to  $\bar{\nu}_\tau$  which can be clearly seen from Fig. 5, but the oscillation probability is small. This is happening due to  $\Delta m_{31}^2 \gg \Delta m_{21}^2$ . Above 10 GeV the oscillation  $\bar{\nu}_e \leftrightarrow \bar{\nu}_{\mu,\tau}$  is suppressed. We observed that above  $E_\nu > 100$  GeV the  $\bar{\nu}_\mu$  does not oscillate to  $\bar{\nu}_\tau$  any more which is similar to the neutrino case discussed above.

The GeV energy neutrinos are produced mostly from the pion decay and have the standard flux ratio at the production point  $\Phi_{\nu_e}^0 : \Phi_{\nu_\mu}^0 : \Phi_{\nu_\tau}^0 = 1 : 2 : 0$  ( $\Phi_{\nu_\alpha}^0$  corresponds to the sum of neutrino and anti-neutrino flux at the source). Also when the muon is damped, the flux ratio at the source is  $0 : 1 : 0$ . The flux observed at a distance  $L$  from the source is given by

$$\Phi_{\nu_\alpha} = \sum_{\beta} \Phi_{\nu_\beta}^0 P_{\alpha\beta}, \quad \alpha, \beta = e, \mu, \tau. \quad (35)$$

When travelling in the Earth, the neutrinos will oscillate and the probability  $P_{\alpha\beta}$  will be different for different flavors which is shown in Fig. 2. By using the above two neutrino flux ratios  $1 : 2 : 0$  (standard) and  $0 : 1 : 0$  (muon damped) at the source, we calculate the normalized observed flux ratio at the IceCube detector for the upward going neutrinos. For this calculation we don't take into account the vacuum effect. Here our main aim is to calculate the observed flux for different flux ratios.

In Fig. 6 we observe that for the flux ratio  $1 : 2 : 0$  at the source the electron neutrino flux  $\Phi_{\nu_e}$  is almost constant at 0.5 and the  $\Phi_{\nu_\mu}$  and  $\Phi_{\nu_\tau}$  oscillate between 0 and 1 averaging out to 0.5. So for this case the observed flux ratio is found to be  $1 : 1 : 1$ . In Fig. 7 we have shown the muon damped scenario. For  $E_\nu > 20$  GeV the  $\Phi_{\nu_e} \sim 0$  but average  $\Phi_{\nu_\mu} \simeq \Phi_{\nu_\tau} = 0.45$ . Again for  $E_\nu < 20$  GeV there are three peaks in the normalized flux for  $\Phi_{\nu_e}$  corresponding to three resonances as discussed before and shown in Figs. 2 and 3. In this case we always get  $\Phi_{\nu_e} < \Phi_{\nu_\mu} \simeq \Phi_{\nu_\tau}$ . Due to lower sensitivity of PINGU  $\sim \mathcal{O}(1)$  GeV it can probe the resonance energy region  $3 \text{ GeV} < E_\nu \leq 12 \text{ GeV}$  very well.

## DISCUSSION

Apart from atmospheric neutrinos, there are other astrophysical sources which can produce low energy GeV neutrinos. By taking into account the realistic Earth density profile, we studied the matter effect on upward going GeV neutrinos. We used the formalism by Ohlsson and Snellman in a varying potential to calculate the neutrino oscillation probability numerically by considering three active neutrino flavors. We observed that in the neutrino energy range  $3 \text{ GeV} < E_\nu \leq 12 \text{ GeV}$  three distinct resonances were observed in three different densities. We also calculated the observed neutrino flux for these upward going neutrinos for standard scenario and the muon damped scenario. For standard scenario we

obtained the observed flux ratio  $1 : 1 : 1$  whereas for muon damped scenario we obtained  $\Phi_{\nu_e} < \Phi_{\nu_\mu} \simeq \Phi_{\nu_\tau}$  for  $E_\nu < 20$  GeV and above this energy we obtained  $\Phi_{\nu_e} \sim 0$ ,  $\Phi_{\nu_\mu} \simeq \Phi_{\nu_\tau} = 0.45$ . The PINGU, which has a lower sensitivity will probably be able to probe this low energy range and shed more light on the MSW mechanism.

We are thankful to Shigehiro Nagataki for many useful discussions. The work of S. S. is partially supported by DGAPA-UNAM (Mexico) Project No. IN110815.

- 
- [1] Y. Fukuda *et al.* [Super-Kamiokande Collaboration], Phys. Rev. Lett. **81**, 1562 (1998) [hep-ex/9807003].
  - [2] Y. Ashie *et al.* [Super-Kamiokande Collaboration], Phys. Rev. D **71**, 112005 (2005) [hep-ex/0501064].
  - [3] M. B. Smy *et al.* [Super-Kamiokande Collaboration], Phys. Rev. D **69**, 011104 (2004) [hep-ex/0309011].
  - [4] A. Gando *et al.* [KamLAND Collaboration], Phys. Rev. D **83**, 052002 (2011) [arXiv:1009.4771 [hep-ex]].
  - [5] F. P. An *et al.* [Daya Bay Collaboration], Chin. Phys. C **37**, 011001 (2013) [arXiv:1210.6327 [hep-ex]].
  - [6] M. G. Aartsen *et al.* [IceCube Collaboration], Science **342**, 1242856 (2013) [arXiv:1311.5238 [astro-ph.HE]].
  - [7] M. G. Aartsen *et al.* [IceCube Collaboration], Phys. Rev. Lett. **113**, 101101 (2014) [arXiv:1405.5303 [astro-ph.HE]].
  - [8] R. Abbasi *et al.* [IceCube Collaboration], Astropart. Phys. **35**, 615 (2012) [arXiv:1109.6096 [astro-ph.IM]].
  - [9] T. Palczewski [IceCube/PINGU Collaboration],
  - [10] T. K. Kuo and J. T. Pantaleone, Phys. Rev. Lett. **57**, 1805 (1986).
  - [11] A. Y. Smirnov, Yad. Fiz. **46**, 1152 (1987).
  - [12] S. T. Petcov and S. Toshev, Phys. Lett. B **187**, 120 (1987).
  - [13] T. Ohlsson and H. Snellman, J. Math. Phys. **41**, 2768 (2000) [J. Math. Phys. **42**, 2345 (2001)] [hep-ph/9910546].
  - [14] T. Ohlsson and H. Snellman, Phys. Lett. B **474**, 153 (2000).
  - [15] T. Ohlsson and H. Snellman, Eur. Phys. J. C **20**, 507 (2001).
  - [16] L. Wolfenstein, Phys. Rev. D **17**, 2369 (1978).
  - [17] S. P. Mikheev and A. Y. Smirnov, Sov. J. Nucl. Phys. **42**, 913 (1985) [Yad. Fiz. **42**, 1441 (1985)].
  - [18] S. Sahu and V. M. Bannur, Phys. Rev. D **61**, 023003 (2000) [hep-ph/9806427].
  - [19] S. Sahu and J. C. D'Olivo, Phys. Rev. D **71**, 047303 (2005) [hep-ph/0502043].
  - [20] S. Sahu, N. Fraija and Y. Y. Keum, Phys. Rev. D **80**, 033009 (2009) [arXiv:0904.0138 [hep-ph]].
  - [21] S. Sahu and B. Zhang, Res. Astron. Astrophys. **10**, 943 (2010) [arXiv:1007.4582 [hep-ph]].
  - [22] A. F. Osorio Oliveros, S. Sahu and J. C. Sanabria, Eur. Phys. J. C **73**, 2574 (2013) [arXiv:1304.4906 [astro-ph.HE]].
  - [23] K. Enqvist, K. Kainulainen and J. Maalampi, Nucl. Phys. B **349**, 754 (1991).
  - [24] M. Freund and T. Ohlsson, Mod. Phys. Lett. A **15**, 867 (2000) [hep-ph/9909501].

- [25] A. M. Dziewonski, D. L. Anderson, *Preliminary reference Earth model*. Phys. Earth Planet. Inter. 25 297-356.
- [26] I. Bartos, A. M. Beloborodov, K. Hurley and S. Márka, Phys. Rev. Lett. **110**, no. 24, 241101 (2013) [arXiv:1301.4232 [astro-ph.HE]].
- [27] S. Gao and P. Meszaros, Phys. Rev. D **85**, 103009 (2012) [arXiv:1112.5664 [astro-ph.HE]].
- [28] S. Adrian-Martinez *et al.* [ANTARES Collaboration], arXiv:1506.07354 [astro-ph.HE].
- [29] V. D. Barger, K. Whisnant, S. Pakvasa and R. J. N. Phillips, Phys. Rev. D **22**, 2718 (1980).
- [30] C. W. Kim and W. K. Sze, Phys. Rev. D **35**, 1404 (1987).
- [31] H. W. Zaglauer and K. H. Schwarzer, Z. Phys. C **40**, 273 (1988).
- [32] S. T. Petcov, Phys. Lett. B **191**, 299 (1987).
- [33] H. Lehmann, P. Osland and T. T. Wu, Commun. Math. Phys. **219**, 77 (2001).
- [34] K. Varela, S. Sahu, A. F. O. Oliveros and J. C. Sanabria, Eur. Phys. J. C **75**, no. 6, 289 (2015) [arXiv:1411.7992 [astro-ph.HE]].
- [35] Y. Ashie *et al.* [Super-Kamiokande Collaboration], Phys. Rev. Lett. **93**, 101801 (2004) [hep-ex/0404034].
- [36] T. Araki *et al.* [KamLAND Collaboration], Phys. Rev. Lett. **94**, 081801 (2005) [hep-ex/0406035].